Physical Communication 35 (2019) 100717

Contents lists available at ScienceDirect

Physical Communication

journal homepage: www.elsevier.com/locate/phycom

Full length article

Multi-UAVs trajectory and mission cooperative planning based on the Markov model☆

Qian Ning [a,b], Guiping Tao [a], Bingcai Chen [c,*], Yinjie Lei [a], Hua Yan [a], Chengping Zhao [a]

[a] College of Electronics and Information Engineering, Sichuan University, Chengdu, 610065, China
[b] School of Physics and Electronics Engineering, Xinjiang Normal University, Urumqi, 830054, China
[c] School of computer science and technology, Dalian University of Technology, Dalian, 116024, China

ARTICLE INFO

Article history:
Received 11 January 2019
Received in revised form 10 April 2019
Accepted 20 May 2019
Available online 23 May 2019

Keywords:
Collaborative mission planning
Trajectory planning
Survival state
Markov model
Meta-heuristic search algorithms

ABSTRACT

As the environment of the battlefield is increasingly complex, single UAV (Unmanned Aerial Vehicle) has trouble in carrying out missions, which requires the cooperation of multiple UAVs. However, search space is very large and search targets are distributed sparsely, and making mission planning and route planning simultaneously is also an NP (Non-Deterministic Polynomial Problems) problem, which makes it extremely difficult in mission planning. Recently, meta-heuristic search algorithms widely used in multi-UAVs collaborative mission planning are difficult to find reliable initial solutions and limit the convergence speed. Aiming at this problem, to take plenty of constraints and performance planning targets in multi-UAV cooperative mission planning problems into full consideration. This paper proposes a two-layer mission planning model based on the simulated annealing algorithm and tabu search algorithm, which solves multi-objectives, Multi-aircraft mission planning problems. This paper combined the five-state Markov chain model with the mission planning model to determine the optimal mission planning scheme by judging the survival state probability of the flight platform. Finally, the simulation results show that this method can greatly improve the survivability of the drone while ensuring optimal mission planning.

1. Introduction

With the rapid development of UAV technology, the UAV has been able to undertake various tasks such as intelligence reconnaissance, battlefield surveillance, electromagnetic interference, air strike, lighting, and damage assessment [1]. Multiple unmanned aerial vehicles (UAVs) cooperative surveillance with a ground station via multihop communications is presented to achieve a tradeoff between surveillance mission and connectivity maintenance in the literature [2]. In literature [3], a multi-targets tracking algorithm based on task allocation consensus is proposed for UAVs to track multiple moving targets under the distributed control architecture in the limited communication range. In literature [4], a coverage search algorithm which is based on the mapping between the basic behavior combination and surroundings is proposed.

Unmanned aerial vehicle (UAV) also can assist BSs to offload the data traffic [5]. The detection of UAVs returned to the podium involves the issue of secure transmission of information [6]. UAV assisted secure transmission [7,8] for scalable videos in hyper-dense networks via caching is studied. In the proposed scheme [9]. The primary transceivers with long distance communicate through the relay [10]. Facing an increasingly complex battlefield environment [11], single UAV can hardly accomplish the designated combat tasks alone, which must be carried out by multiple UAVs with coordination [12]. The key to multi-UAV collaborative mission planning is the task assignment, which assigns different missions to different UAVs to optimize the operational effectiveness of the whole fleet and minimize the operational cost. The method of mission planning mainly includes global search algorithm, dynamic programming algorithm, Hungarian algorithm [13] and soft computing method. In recent years, various soft computing methods have been frequently used to solve mission planning. Each "mission" area has been refined into multiple targets, which need to be illuminated and struck simultaneously. The area may also contain no-fly zones. Such as threats (SAM, etc.), as well as buildings that do not appear in areas with collateral damage (such as schools, hospitals, etc.) [14].

UAV collaborative mission planning and route planning are two essential sections for multi-UAV mission planning. Besides,

☆ This work was supported in part by the National Natural Science Foundation of China under Grant 61771089, in part by the Open Research Fund of Key Laboratory of Wireless Power Transfer, Ministry of Education and in part by the Open Research Fund of Key Laboratory of Data Security, Xinjiang Normal University under Grant XJNUSYS102018B01.

* Corresponding author.
E-mail address: china@dlut.edu.cn (B. Chen).

https://doi.org/10.1016/j.phycom.2019.100717
1874-4907/

the two parts are nondeterministic polynomial (NP) problems [15, 16]. The solution is too difficult to implement, and the exhaustive method or the optimal control method will cost a lot of time on calculation. In order to reduce the difficulty of solving, the problem is usually divided into two sub-problems: collaborative mission planning and route planning. Weakening or not considering the coupling between them, using layered decoupling to solve them separately [17–22]. The commonality of these solutions is to separate the two problems. The kinematic constraints, environmental obstacles and threat zone constraints of the flight platform are not considered when the mission planning is in progress, only the timing constraints and interaction between missions are considered. The results of mission planning are considered as the input of route planning to get a smooth track that satisfies UAV's own constraints, obstacles, threat zones, and collision avoidance constraints. The difficulty of solving the problem is reduced by the hierarchical solution method. However, the actual mission environment is usually time-varying and uncertain, while the settlement process of the hierarchical solution method is asynchronous, besides the search time is too long in complex environments. Moreover, while guaranteeing the highest total effect value, the survival probability of the aircraft cannot be guaranteed, but the survival probability of UAV will affect the total effect value of mission execution in turn.

As for these problems, the Markov state model mentioned in the literature [23] and the state transition and cost calculation in the literature [24] are introduced. To grasp the specific survival probability of the UAVS during flight, on which the search is modified to match the particle swarm algorithm [25]. Before entering the mission area, the genetic algorithm [26,27] is used to obtain the shortest path which traverses all target points. The simulated flight platform passes the shortest path through each target point to evaluate the survival state probability. To set a threshold value of the state probability of being hit, the pre-processing is performed to determine whether the target point is executed. After the pre-processing is completed, the multi-UAV collaborative mission planning strategy based on the Tabu search algorithm [28,29] and simulated annealing algorithm is used to obtain the execution sequence of each target in the mission area to achieve the best strike effect, the shortest total task execution time or shortest total distance.

2. Problem setting

Our model consists of two parts: based on Markov model, using the genetic algorithm to get the shortest path which traverses all targets to perform a pretreatment; mission planning through tabu search algorithm and simulated annealing algorithm.

2.1. Markov survival state model

Markov model with continuous time and discrete state is used to modeling UAV survival states and their transfer. In this paper, five survival states are discussed [30]. The state probability and survival cost of the UAV are obtained according to state transition strength and transfer cost set in different regions. In the survival cost part of route planning, compared with traditional methods, the greatest advantage of using this model is that the survival cost and the state of the UAV flight can be visualized. The following is a detailed description of the five states, transfer strength and survival cost calculations:

2.1.1. Five states of the survival model

There are five states of the UAV, which are undetected (U), detected (D), tracked (T), engaged with the enemy (E), and hit (H) [31]. The state transition can only occur between two adjacent states, and the transition is reversible. For example, when the UAV enters the range of the enemy detection radar, the aircraft will have a certain probability to be converted from state U to State D, and there is also a certain probability of transitioning from state D back to U when the aircraft flies back to the safe zone. It is important to note that only state H does not have reversibility, which means that if the aircraft moves to the hit state, it will always be in that state.

2.1.2. Transfer strength setting

Since state transitions can only occur between adjacent states, there are seven state transitions for the five-state models, and the transfer strength implies the probability that a particular point in space will move from one state to another. λ_{ij} is used to represent the transfer strength from state i to state j. In order to highlight the impact of different threat coverage areas and safety areas on the aircraft, different transfer strengths need to be set for them. For example, only within the detection radar coverage, the aircraft has the possibility to be detected and tracked, so the value of λ_{UD}, λ_{DT}, λ_{TD}, λ_{DU} are greater than 0. When there is no weapon radar in the detection radar. The probability of the aircraft leaving the engagement state is greater than 0. Fig. 1 shows all state transition strengths of the transition in the safe area, the detection radar and the weapon radar.

The value of the transfer strength is set to be inversely proportional to the distance from the threat center. λ_{oij}, λ_{sij}, λ_{wij} respectively indicate the maximum transfer intensity value from the state i to the state j in the area of the safe area, the detection radar, and the weapon radar. Since different radars have different functions, the transfer strength between states in different types of radar regions will be different. The transfer intensity value of point p is as shown in Eq. (1). This setting ensures that the closer the aircraft is to the center of threat region, the transfer strength value will be higher.

$$\lambda_{ij} = \begin{cases} \lambda_{oij}, & p \notin S, p \notin W \\ \dfrac{r-d}{r}\lambda_{sij}, & p \in S, p \notin W \\ \dfrac{r-d}{r}\lambda_{wij}, & p \in W \end{cases} \tag{1}$$

where r is the radius of threat, d is the Euclidean distance between the aircraft and the threat center, and Sensor and Weapon represent the radar and weapon radar areas.

2.1.3. Calculation of transfer intensity in overlapping regions

It is very likely that the enemy will distribute the detection radar and the weapon radar in space in the form of overlapping, and provide threat information to the weapon radar through the detection radar. Since multiple radars covering the same area are easier to detect and track than a single radar, assuming that the radar detects the aircraft independently of each other, the state of being detected, not being detected and being tracked can be seen as the sum of the independent Poisson processes. At the same time, for the overlapping areas of multiple radars, the probability of the aircraft getting rid of being tracked should be less than the single radar coverage area. In which case the radar coverage area can be regarded as a parallel component system. The possibility of being engaged or being hit does not due to the number of overlapping radar zones, so it is usually to choose the

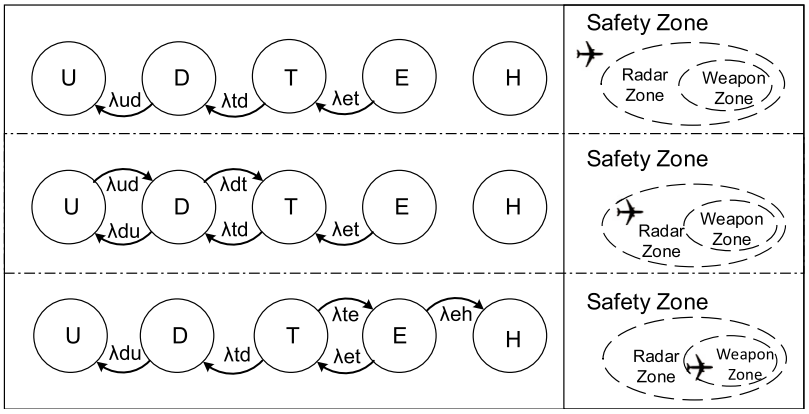

Fig. 1. State transition strength setting.

worst case [32].

$$\lambda_{ij}^{c} = \begin{cases} \lambda_{ij}^{1} + \lambda_{ij}^{2} & (i,j) = (U,D)\&(D,T) \\ max(\lambda_{ij}^{1}, \lambda_{ij}^{2}) & (i,j) = (T,E)\&(E,H) \\ \dfrac{\lambda_{ij}^{1}\lambda_{ij}^{2}(\lambda_{ij}^{1} + \lambda_{ij}^{2})}{\lambda_{ij}^{1}\lambda_{ij}^{2} + (\lambda_{ij}^{1})^2 + (\lambda_{ij}^{2})^2} & (i,j) = (D,U)\&(T,D), \in D \\ min(\lambda_{ij}^{1}, \lambda_{ij}^{2}) & (i,j) = (D,U)\&(T,D), \notin D \\ min(\lambda_{ij}^{1}, \lambda_{ij}^{2}) & (i,j) = (E,T) \end{cases} \quad (2)$$

In summary, the calculation method for the transfer intensity of the overlap region is as shown in the formula (2), λ_1, λ_2 represent as the transfer intensity value the region 1 and the region 2.

2.1.4. State probability setting

The state probability provides important decision support for the UAV. In order to calculate the change of each state probability of the UAV on the route with time, the Markov chain framework is applied, firstly the transfer intensity matrix $\Lambda(t)$ is constructed and then to solve the differential equation shown in (3) to obtain the state probability vector p(t).

$$\vec{p}(t) = \Lambda^{T}(t)p(t) \quad (3)$$

Since the state of the survival model is only five, the state is finite, and $\Lambda(t)$ is a constant matrix in a certain period of time, Eq. (3) can be solved by the iterative method shown in (4).

$$p(t_n) = e^{\Lambda_{n-1}^{T}(t_n - t_{n-1})}p(t_{n-1}) \quad (4)$$

In the formula (4), the matrix index needs to be solved, and the solution method of the matrix index is shown in formula (5).

$$e^{\Lambda} = \sum_{n=0}^{\infty} \frac{(\Lambda)^n}{n!} \quad (5)$$

2.2. The shortest path of mission planning

Learning from the theory of biological evolution, the genetic algorithm simulates the problem into a biological evolution process, to generate the next generation solution through genetic, crossover, mutation, natural selection, etc. Gradually, to eliminate the solution with low fitness function value to increase the fitness solution. After the evolution of the N generation, it is very likely that individuals with high fitness function values will evolve.

The design steps for the genetic algorithm improves the TSP (Traveling salesman problem) problem are shown as follows.

1. Initialize parameters;
2. Randomly generate an initial population of a group of individuals and evaluate the adaptation value of each individual;
3. Determine whether the convergence criterion of the algorithm is satisfied (here is the number of iterations). If satisfied, then output the search results, otherwise, execute step [4–8];
4. Perform a selection operation (randomly select two population individuals), use the idea of roulette selection, and randomly return the subscript of an individual in the current group according to the probability size;
5. Cross operation is performed according to the probability of hybridization const double $P_C OPULATION = 0.8$;
6. which is smaller than the mutation probability $P_l NHERIATANCE$, and is subjected to mutation processing (randomly swap the positions of two target points);
7. Update the path of $Son_s olution[]$ and $Calc_P robability(G, total_l ength)$;
8. Update the group with the "father and son mix selection" (elite retention strategy);
9. Return to step 2 to determine whether to perform the next iteration.

2.3. The synergistic mission planning model

The target of synergistic mission planning is not only to ensure the attack effect but also to make the flight as short as possible. The model is established as shown in formula (6).

$$max \sum_{r=1}^{R} \sum_{(i.j)\in A} \chi^{r} c_{ij}^{r} - \omega L, \quad \chi^{r} = \begin{cases} 0, & x_{ij} \neq r \\ 1, & x_{ij} = r \end{cases} \quad (6)$$

R is the number of collaborative mission plane, A is the path set, i and j represents the start point and the end point of a certain path respectively. c_{ij}^{r} is the attack effect value of the aircraft r through the (i,j) segment path. L represents the total distance of flight. ω is the coefficient used to balance the impact of the attack effect and the total distance on the result.

The decision variable of the model is a matrix of size n*n, R is the number of all nodes in the number of the mission scenario that contains entrance and exit. The value of x_{ij} indicates a serial number of aircraft passing through the path from node (i) to the node (j). In fact, in order to better express the constraints of the model, the decision variable should be set to a three-dimensional binary variable of R * n * n, but in order to compress the scale of the decision variable and improve the efficiency of the solution in the simulation, the following methods are adopted: $x_{ij} = r$ means

that the aircraft passes the (i,j) segment path, $x_{ij} = 0$ means that no aircraft passes the (i,j) segment path. And in the expression of the model and subsequent constraints, x^r is used to transfer the decision variable x_{ij} to an $R \times n \times n$-dimensional binary variable.

According to the requirements of the mission area planning, the constraints are as shown in Eqs. (7) - (15):

$$\sum_{(o,j)\in A} x_{oj} = \sum_{r=1}^{R} r \tag{7}$$

$$\sum_{(i,d)\in A} x_{id} = \sum_{r=1}^{R} r \tag{8}$$

$$\sum_{(i,k)\in A} x_{ik} - \sum_{(k,j)\in A} x_{kj} = 0,\ k \in N \setminus \{o, d\} \tag{9}$$

$$\sum_{m\in M} \sum_{s\in S_m} \sum_{(i,j)\in A_s} \varphi_m \chi^r \le \Phi,\ r \in [1, R] \tag{10}$$

$$\sum_{r=1}^{R} \sum_{s\in S_m} \sum_{(i,j)\in A_s} \chi^r = 1,\ m \in M \tag{11}$$

$$\sum_{r=1}^{R} \sum_{s\in S_m} \sum_{(i,j)\in I_s} \chi^r = 1,\ m \in M \tag{12}$$

$$\sum_{r=1}^{R} \sum_{(i,j)\in A_s} \chi^r - \sum_{r=1}^{R} \sum_{(i,j)\in I_s} \chi^r = 0,\ s \in S \tag{13}$$

$$\sum_{i\in N_m^A} t_i = t_m^A,\ \sum_{i\in N_m^I} t_i = t_m^I,\ m \in \tag{14}$$

$$t_m^A \cap t_m^I \neq \varnothing,\ m \in M \tag{15}$$

Eqs. (7) - (8) require each aircraft must fly into the area from the entrance, and fly out the area from the exit. O represent the entrance node and d represents the exit node. Eq. (9) guarantees the continuity of each flight. N represents the set which includes entrance, exit, and all other nodes. Due to the limit of the number of weapons each aircraft can carry. Eq. (10) requires the number of weapons each aircraft can use no more than the maximum of weapon each aircraft carrier. M is the set of targets, S_m is sector set of target m, A_s is the path set of nodes which destination is attack node. ϕ_m is the number of weapons that attack node m needs. ϕ is the maximum number of weapon that aircraft r can carry. Eqs. (11), (12) guarantee each target to be attacked and illuminated only once. I_s is the path set of nodes which destination is illumination node. Eq. (13) describes the spatial synchronization of illumination and attack. S is the set of all sectors. Eqs. (14)–(15) describe the synchronization of illumination and attack in time, but also guarantee an illumination node and an attack node to be activated only by one target. N_m^A and N_m^I represent the set of attack nodes and illumination nodes for target m respectively. t_m^A and t_m^I represent target m whose range of access time of being attacked and illuminated respectively. t_i is the range of access time for node i. The same goal whose range of time of being attacked and illuminated are required to have an intersection.

2.3.1. Model solving method for collaborative mission planning

According to the above, it can be seen that the size of decision variables [33] is very large. Take the scenes of the three targets shown in Figure 2.1 as an example. There are 13 available sectors, including for the entrance and exit 41 nodes in total. Decision variables have a scale of more than 1600 dimensions and more than 1500 constraints. When the number of targets increases, the scale will grow geometrically. The traditional linear programming method is undoubtedly inefficient and difficult to implement, for the reason that this paper uses a meta-heuristic search algorithm to pursue efficient optimization Results.

The existence of a large number of constraints leads to a huge number of solutions, but the proportion of feasible solutions is very small. If a population-based random search algorithm is adopted, such as PSO (Particle Swarm Optimization), it is very easy to fall into a local optimum. Therefore, an individual-based meta-heuristic search algorithm is adopted. Setting each individual's neighborhood will greatly reduce the work on invalid solutions.

At the same time, in order to further narrow the scale of the target, for three parts of the collaborative mission planning, a nested search strategy is adopted. The determination of the sector is divided into the search outer layer portion, while the target allocation is divided into the search inner layer portion. When the sector is determined, the number of available nodes including the entrance and exit is reduced to 11, while the scale of the decision variable is reduced from 1600 to 150, search efficiency can be effectively improved. The outer and inner layers respectively use the following search algorithm.

2.3.2. Out layer based on the taboo search algorithm

The taboo search algorithm obtains the optimal neighbor as a new solution by searching the neighborhood of the current solution and prevents the loop search through the taboo table. In the determination of the sector, the sector of each target is selected as the search target, as shown in Eq. (16):

$$X = [s_1, s_2, s_3, \ \dots\ , s_M],\ s_i \in [1, \lambda_i] \tag{16}$$

x represents the result of the outer search, M is the number of targets, s_i is the sector number activated by target i, λ_i is the sector number of target i. Each target contains 6 sectors theoretically. Some sectors are not allowed to be activated for the reason that there are civil buildings in the scene. λ_i is the number of available sectors.

The neighborhood of the current sector s_i of the target i is the first available sector on the left side and the first available sector on the right side, as shown in the left side of Fig. 2, the shaded part is the current sector, whose neighborhood is the gray part. After multiple targets are combined, the neighborhood of the current sector of one target is obtained each time, while the rest of the target sectors are fixed. Take the scenario of 2 targets as an example, each solution should have 2^2 neighborhoods. Neighbors are shown specifically in Fig. 2.

The scale of the solution in this problem is not large, so the search object is directly used as a taboo object. The optimal solution generated by each iteration is used as a new solution for the next iteration, which will be stored in the taboo table. The first we should confirm whether this solution lies in the taboo table before we take it as a new solution. In addition, the setting of the taboo length is proportional to the number of targets in the scene. More targets, the taboo length will be longer to prevent the search from falling into a circulation.

The steps of the tabu search for the problem of sector determination are as follows:

1. Initialize the solution, set the sector of each target to 1, and store it in the taboo table, the taboo length is set to three times the number of targets;
2. Search all the neighbors of the current solution that are not tabooed, then calculate the fitness value, the optimal neighbor will be the new solution;
3. Store the new solution in the taboo table, update the iterations stored the taboo table, and unblock the object whose iterations reaches the taboo length;
4. Meet the iteration end condition, then exit, otherwise return to step 2.

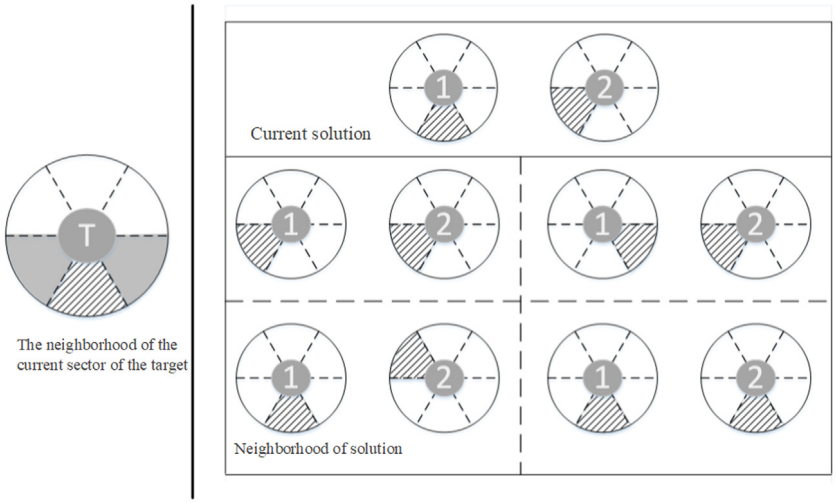

Fig. 2. Neighborhood setting graph of taboo search in section determination problem.

2.3.3. Inner layer based on simulated annealing algorithm

After the outer sector is determined, the scale of the target allocation problem remaining in the inner layer is reduced to m*m. There are only 3 nodes each target has after sector determined, so m = 3t+2, t is the number of targets. Despite that, the search space is still very large. With 3 targets and 4 aircraft as an example, there is 4^{121} kinds of solution, but only 28 million effective solutions. For the trait that the search space is very large and the proportion of effective solutions is very low, as well as easy to fall into a local optimum. The inner search algorithm uses a simulated annealing algorithm, which is based on the individual generation of perturbation solutions and can accept relatively inferior solutions with a certain probability, which makes it more than other search algorithms. The high probability jumps out of the local optimum and converges to the global optimal solution. Therefore, simulated annealing is very suitable for the characteristics of the spatial search of the inner search solution.

2.3.4. Generation of perturbation solutions

In the inner search problem, the generation method of the simulated annealing disturbance solution is very important. The traditional disturbance method has a single variable of the disturbance solution, or randomly exchanges the values of two variables. The problem of low search efficiency caused by large search space and extremely low effective solution ratio cannot be solved.

According to the actual situation of the problem, the paper divides the generation of the disturbance solution into three parts as follow: (1) the change of the aircraft combination; (2) the change of the illumination node; (3) the change of the target attack sequence. The change of the aircraft combination refers to the change of the combination of the attack and the illumination of the aircraft. The change of the illumination node refers to the change in the direction of the illumination path. Both of the above methods are for a single target selected randomly. The above three changes cover all possible effective solutions. Each time the disturbance solution is generated, one of the three methods is randomly selected according to a certain probability. The rest remains unchanged. Due to the number of aircraft combinations changes is very large, therefore this method will occupy a large proportion of three methods. A perturbation solution is generated according to the aircraft combination, illumination nodes, attack sequence and the sector information determined by the outer layer. This purposeful random disturbance makes the simulated annealing more efficient compared with the random disturbance of a single variable or the random exchange of multiple variables.

The objective function of the inner search algorithm is as follow:

$$f(x) = \begin{cases} -\left(\sum_{r=1}^{R} \sum_{(i,j)\in A} \chi^r C_{ij}^r - \omega L\right) \\ C_{max} \end{cases} \tag{17}$$

In Eq. (17), the formula above is chosen when x is an efficient solution, the below formula is chosen when x is not an efficient solution.

If the solution satisfies all the constraints in (7) - (15), then it is an effective solution. If any constraint is violated, it is an invalid solution. C_max is the penalty coefficient of invalid solutions, which usually take a large positive integer value.

In summary, the simulated annealing search steps for inner target allocation are shown as follows:

1. Initialize, randomly generate the target attack sequence, the aircraft combination and the lighting node to generate an initial solution according to the outer search result, set an initial temperature T = 100;
2. Randomly select a perturbation method according to a certain probability, generate a perturbation solution, and accept the perturbation solution according to the Metropolis criterion;
3. Satisfy the iterative end condition at the current temperature, progress step 4; otherwise, return to step 2;
4. Lower the temperature, if the temperature has dropped to the lowest temperature, the search ends and the result is returned; otherwise, return to step 1.

In the high-temperature search stage of simulated annealing, the probability of accepting a worse disturbance solution is larger, and the solution in the large range neighborhood of the current solution can be accepted. Therefore, this stage is mainly the horizontal search stage. Lower the temperature becomes, the probability of inferior disturbance solutions will become smaller, which is the process of gradual convergence to the global optimal solution.

3. Simulation results and analysis of cooperative mission planning based on integrated Markov model

The effects of tabu search and simulated annealing based on the Markov model on mission planning were proved to be a safe and efficient method. These results suggested that the viability

Table 1
Integrated scene position parameter table.

Name	Start point (x,y,z)	End point (x,y,z)	Detection radar (x,y,z,r)	Weapon radar (x,y,z,r)
Coordinate	(840, 550, 4)	(800, 650, 4)	(520, 510, 4, 130) (675, 750, 4, 135) (860, 530, 4, 150)	(700, 650, 4, 60) (620, 550, 4, 60) (950, 680, 4, 60)
Name	Target (x,y)	Civil building (x,y)	Enemy defense System (x,y)	
Coordinate	(870, 585) (940, 595) (920, 645)	(870,580) (870,592) (865,687) (920,639)	(932,600) (940,605) (947,600) (945,589) (1010,649)	

Table 2
Transfer intensity of survival model.

	λ_{UD}	λ_{DU}	λ_{DT}	λ_{TD}	λ_{TE}	λ_{ET}	λ_{EH}
Outside of threat	0	0.2	0	0.2	0	1	1
Detection radar	0.4	0.1	0.3	0.1	0	1	0
Weapon radar	0	0.2	0	0.2	0.2	0.1	0.3

of UAVs significantly increased When the drones make route planning and mission planning simultaneously.

3.1. Parameter settings

The scenario integrates the dynamic route planning and collaborative mission planning. The parameter settings in the simulation are set in Table 1.

Table 2 shows the setting of the state transition strength in the Markov survival model applied to the simulation experiment. It can be seen from the table that the aircraft has the probability of being detected and tracked in a single detection radar and will not be attacked, when the aircraft is in a single weapon radar, the aircraft will not be detected and tracked, but the aircraft will be transferred to the state of engagement and there is a certain probability of damage.

3.2. Integrated scene simulation

The integrated scene is shown in Fig. 3, which consists of two parts: the dynamic route planning and collaborative mission planning. The dynamic route planning part is mainly distributed from the starting point and the entrance of the mission area and from the exit of the mission area to the end of the scene, which mainly uses PSO (Particle Swarm Optimization) algorithm for route planning. This paper mainly introduces the mission planning, so the route planning will not be explained here.

3.3. The shortest path of mission planning

After establishing the Markov survival state model in the mission area, the state of the flight platform at each moment is related to the state of the previous, so the calculation of the state probability of flight platform is related to the trajectory of aircraft. In the mission area, the TSP (Traveling salesman problem) problem is improved by genetic algorithm to get a get the shortest path which traverses all target points as shown in Fig. 4.

According to the flight platform, the flight path traverses all the target points along the shortest path to perform a pre-processing to obtain the state probability values of the aircraft when each target point is passed. Since the state probability value of the task target points being shot down is large, it will affect the execution of the next task target point. Thence we first perform a pre-processing before the mission planning, set a threshold of

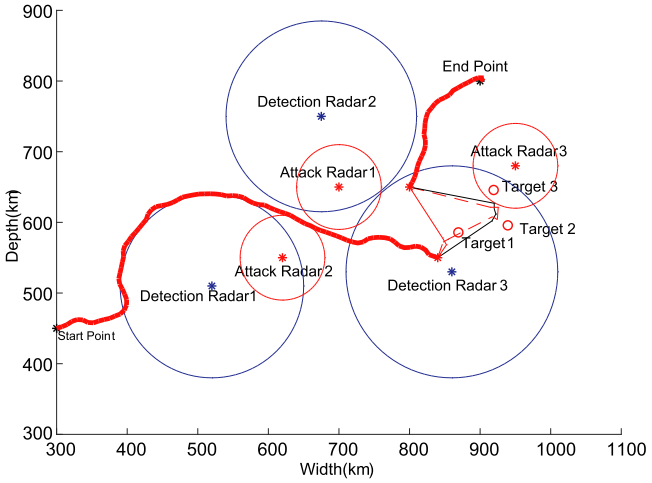

Fig. 3. Results of integrated dynamic route planning and collaborative mission planning.

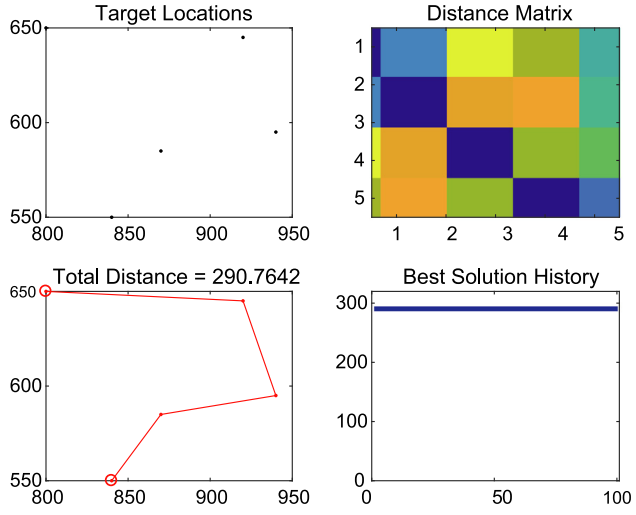

Fig. 4. Genetic algorithm to find the shortest path result graph.

the probability value of being shot down to determine whether the target point to be executed. This ensures a higher degree of completion of the entire task.

3.4. Mission planning based on Markov model

From Table 3, we can see that when the flight platform passes the target point 3, the probability of being shot down is very

Table 3
State probability value of each target point of the flight platform along the shortest path.

	Undetected	Detected	Track	Engage	Hit
Start point	0.0084	0.6268	0.3648	0	0
Target1	0.0328	0.5537	0.4135	0	0
Target2	0.0419	0.5483	0.4098	0	0
Target3	0.0016	0.0561	0.0223	0.1636	0.7314
End point	0.0173	0.5156	0.4671	0	0

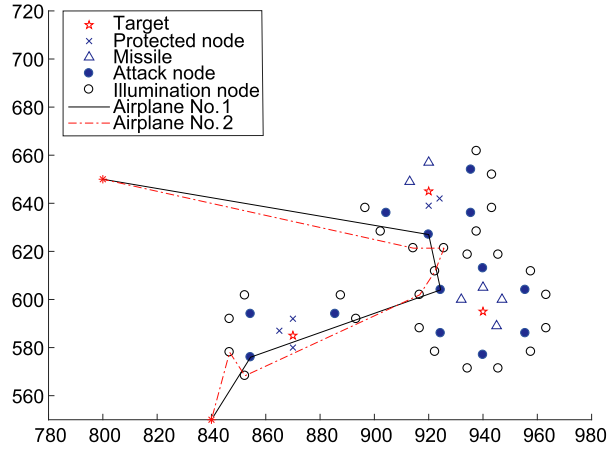

Fig. 5. Mission assignment result graph without Markov model.

high, if the aircraft passes through target point 3, there is a great risk of being shot down and affecting the next mission execution, comprehensive task completion priority perspective, we give up the implementation of target point 3, and then task planning. We can compare Fig. 5 with Fig. 6. Fig. 5 shows the mission planning without the Markov survival state model. Therefore the impact of detection radar and weapon radar on the survival state of the aircraft is not considered, the outer layer is directly executed according to the mission plan. The tabu search performs sector determination, and the inner layer of the mission plan performs simulated annealing to perform target allocation. Fig. 6 shows that the Markov survival state model has been added. We can see from the figure that the mission planning does not involve the mission target point 3, for the reason of the high risk of target 3 that the target point 3 is abandoned in mission planning. The comparison results show that the mission planning with Markov model improves the overall mission completion and the flight platform's survival rate.

3.5. Collaborative task planning simulation results and analysis

In order to explain the closeness of the results obtained by the strategy and optimal solution, the comparison experiment uses the method of traversing all the effective solutions to obtain the optimal solution of the scene and compares the running time of the two methods. The simulation results are as follows.

3.5.1. Parameter setting

In all scenario simulation experiments, it is assumed that the maximum number of weapons that can be carried by all aircraft is 2, and the number of weapons required to attack each target is 1 for each aircraft. Assume that the ideal attack effect E is 1, the weakening coefficient μ is 0.85, the inner layer simulated annealing initial temperature is 100, and the search iteration is 40 times at each temperature. The generation method of the three kinds of disturbance solutions of the aircraft combination, the lighting node, and the attack sequence is set. For 4:3:3, the

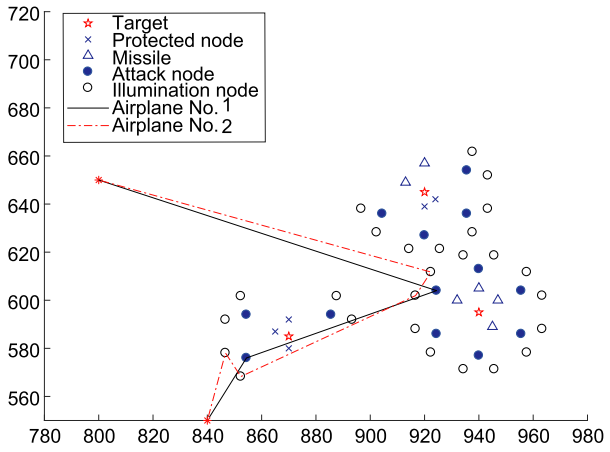

Fig. 6. Task assignment result based on Markov model.

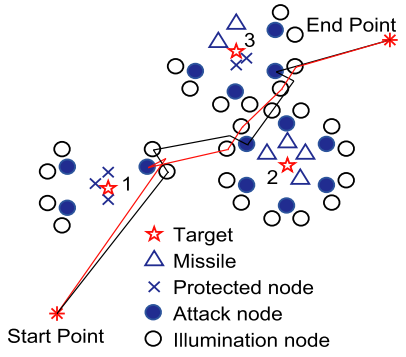

Fig. 7. 3-target and 2-aircraft.

penalty coefficient in the fitness function is set to 10000; the outer taboo searches for the maximum number of iterations of 200, and more than 15 times the global optimization is not updated to stop the iteration.

In the resulting graph, the blue hollow circle and the black hollow circle respectively represent the attack node and the illumination node; the target number will be numerically marked in the figure, △ is the enemy defense, and the scope of the defense is marked in a circle. × is a civil building; the lines of different states indicate the flight paths of different aircraft, and the simulation results will show the direction of the weapon strike for each target with arrows.

3.5.2. Results and analysis

The simulation results of using 2 and 4 aircraft in the 3 target scenarios are shown in Figs. 7 and 8. In Fig. 7, due to the existence of civil buildings, the north, south, and southwest directions of target 1 are not allowed to attack. The target north is not allowed to attack from north to northwest, and because of the limitation of aircraft carrying weapons, target 1 and target 2 are One of the aircraft attacks, the other aircraft illuminates, and the function of the two aircraft is exchanged when attacking the target 3. In addition, it can be seen that the attack position for the southwest direction of the target 2 should have the best attack effect, but due to the flight The reason for the distance is to choose the northwest azimuth attack, which makes the attack effect weaker. The target 2, target 3 use the same aircraft for attack, target 2 uses another aircraft attack, the other two The frame is only used as lighting.

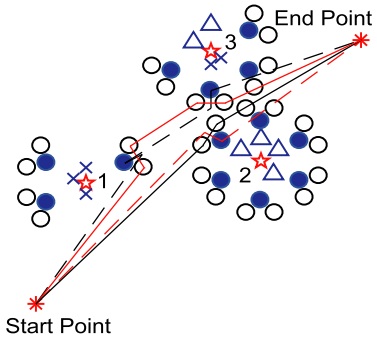

Fig. 8. 3-target and 4-aircraft.

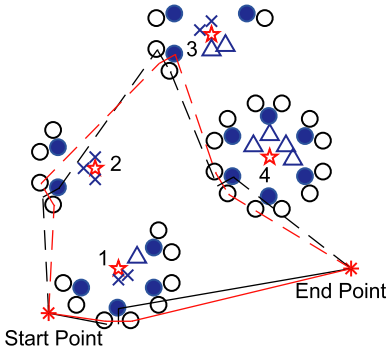

Fig. 11. 4-target and 4-aircraft.

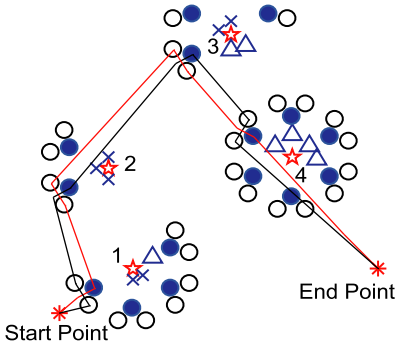

Fig. 9. 4-target and 2-aircraft.

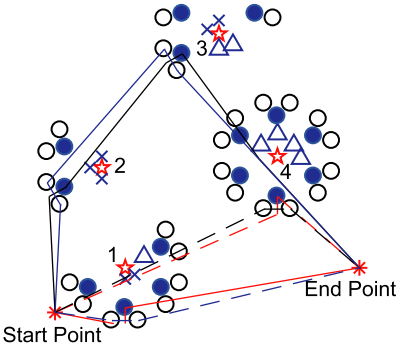

Fig. 12. 4-target and 6-aircraft.

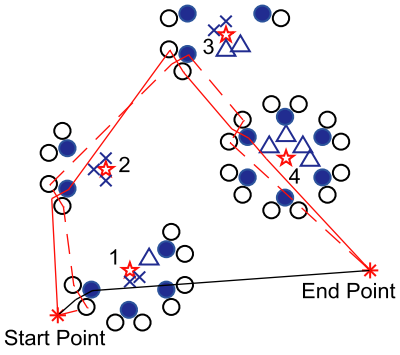

Fig. 10. 4-target and 3-aircraft.

Table 4
Simulation result Different scene.

Target	Aircraft	Optimal fitness value	Total flight	Total attack effect	Running time (s)
3	2	−32.89	357.43	2.85	14.90
	3	−50.47	533.17	2.85	16.67
	4	−67.94	707.85	2.85	29.12
4	2	−47.36	512.10	3.85	44.97
	3	−59.78	636.39	3.85	63.86
	4	−73.26	771.13	3.85	86.58
	5	−88.69	926.90	3.85	50.84
	6	−104.30	1083.0	4.00	59.70
5	3	−67.40	722.56	4.70	70.51
	4	−71.73	765.80	4.85	140.13
	5	−88.73	935.84	4.85	143.34
	6	−102.47	1071.7	4.85	101.48
6	3	−88.89	947.45	5.85	138.81
	4	−97.80	1036.5	5.85	154.74
	5	−107.16	1130.1	5.85	212.01
	6	−117.63	1234.8	5.85	197.55

The simulation results of using 2, 3, 4, and 6 aircraft synergies in the 4 target scenarios are shown in Figs. 9 to 12 respectively. In the scenario of 2 flying, 3 and 4 aircraft, the target attack order is 1-2-3-4, while in the case of 6 aircraft, the target order is 1-2-4-3; for 2 aircraft Scene, target 1, target 3 use the same aircraft attack, target 2, target 4 use another aircraft to attack, satisfying the constraint of carrying at most 2 weapons per aircraft; attack orientation, due to voyage, target 4 It was not attacked at the location with the best attack effect; the aircraft of the three aircraft had an extra plane, which was used for the attack on target 1, and then directly flew to the exit.

In the scene of 4 and 6 aircraft, the aircraft formations are combined in pairs. In the simulation results of the 4 aircraft, one group of aircraft performs targets 2, 3, and 4 and alternately acts as an attack and lighting. The other group of aircraft completes the target 1 and directly reaches the exit; 6 aircraft planes form three groups of aircraft cooperation Perform lighting and attack on Goal 1, Goals 2, 3, and 4. And it can be seen that in all the result graphs, the path between the nodes is the shortest path to avoid the enemy defense, and it is obvious that the flight path of the aircraft directly reaching the exit after completing the target 3 in Fig. 12.

In Table 4, the simulation results of the collaborative mission planning obtained by using different numbers of aircraft from the target 3 to the target 6 scene are sequentially displayed. The results list the fitness values corresponding to the optimal solution obtained by the search, the total range of all aircraft, the overall attack effect value, and the time the program is running.

It can be seen from Table 4 that as the number of targets in the scene increases, the running time also increases. The reason for that is the number of neighbors of each solution in the outer search increases due to the increase of the target; while in the same scenario, it runs. Most of the time increases with the number of aircraft. This is because the number of aircraft directly affects the number of possible aircraft combinations. In general, the increase in the number of aircraft will lead to the process of obtaining the global optimum. It becomes slow, and of course, there is a certain probability that a global optimal is obtained quickly.

4. Conclusion

In this paper, the problem of heterogeneous aircraft formation collaborative mission planning is described in detail, and a large number of constraints and performance planning objectives in multi-UAV collaborative mission planning are fully considered. An improved simulated annealing algorithm and tabu search algorithm are proposed. The two-layer mission planning model solves the task planning problem of multi-target and multi-aircraft. At the same time, the task model is further combined with the Markov chain model. Before the mission planning, the survival state probability of the flight platform is judged by preprocessing, thereby optimizing the mission planning scheme and improving the survival rate of the aircraft. This method combines route planning issues with mission planning to some extent, the various factors that affect the flight platform takes into account. In response to this NP problem, we need to further explore a more optimized solution.

Conflict of interest

None.

Declaration of competing interest

The authors declare that they had no conflict of interest with respect to their authorship or the publication of this article.

References

[1] D.T. Brown, Routing Unmanned Aerial Vehicles While Considering General Restricted Operating Zones, Ohio: Air Force Institute of Technology, 2001.
[2] Q. Zhu, R. Zhou, J. Zhang, Connectivity maintenance based on multiple relay UAVs selection scheme in cooperative surveillance, Appl. Sci. 7 (1) (2017) 8.
[3] Y. Cui, J. Ren, W. Du, et al., UAV Target tracking algorithm based on task allocation consensus, J. Syst. Eng. Electron. 27 (6) (2016) 1207–1218.
[4] Z. Chen, Y. Lu, Z. Hou, et al., UAV'S coverage search planning algorithm based on action combinations, J. Shanghai Jiaotong Univ. 24 (1) (2019) 48–57.
[5] Fen Cheng, Shun Zhang, Zan Li, Yunfei Chen, Nan Zhao, F.Richard Yu, Victor C.M. Leung, UAV Trajectory optimization for data offloading at the edge of multiple cells, IEEE Trans. Veh. Technol. 67 (7) (2018) 6732–6736.
[6] Yang Cao, Nan Zhao, F.Richard Yu, Minglu Jin, Yunfei Chen, Jie Tang, Victor C.M. Leung, Optimization or alignment: Secure primary transmission assisted by secondary networks, IEEE J. Sel. Areas Commun. 36 (4) (2018) 905–917.
[7] Nan Zhao, Bingcai Chen(*), Joint optimization of power splitting and allocation for SWIPT in interference alignment networks, Phys. Commun. 29 (8) (2018) 67–77.
[8] Bingcai Chen, Zhenguo Gao, Manrou Yang, Qian Ning, Chao Yu, Weimin Pan, Mei Nian, Dongmei Xie, Packet multicast in cognitive radio ad hoc networks: A method based on random network coding, IEEE Access 6 (1) (2018) 8768–8781.
[9] Nan Zhao, Fen Cheng, F.Richard Yu, Jie Tang, Yunfei Chen, Guan Gui, Hikmet Sari, CaChing UAV assisted secure transmission in hyperdense networks based on interference alignment, IEEE Trans. Commun. 66 (5) (2018) 2281–2294.
[10] Bingcai Chen, Yu Chen, Yunfei Chen, Yang Cao, Nan Zhao(*), Zhiguo Ding, A novel spectrum sharing scheme assisted by secondary NOMA relay, IEEE Wirel. Commun. Lett. 7 (5) (2018) 732–735.
[11] Nan Zhao, Weidang Lu, Min Sheng, Yunfei Chen, Jie Tang, F.Richard Yu, Kai-Kit Wong, UAV-Assisted emergency networks in disasters, IEEE Wirel. Commun. 26 (1) (2019) 45–51.
[12] M. Alighanbari, Task Assignment Algorithms for Teams of UAVs in Dynamic Environment, Massachusetts: Massachusetts Institute of Technology, 2004.
[13] Peng Chen, Li Jianli, Wang Qi, Firepower assignment by improved hungarian algorithm based on ad hoc networks, J. Projectiles Rockets Missiles Gui-dance 34 (5) (2014) 169–172, 179 environments. Journal of Intelligent & Robotic Systems, 2013, 70(1-4): 303-313.
[14] N.H. Quttieh, T. Larsson, K. Lundberg, et al., Military aircraft mission planning: a generalized vehicle routing model with synchronization and precedence, Euro. J. Transp. Logist. 2 (1–2) (2013) 109–127.
[15] L.F. Bertuccelli, Robust Decision-Making with Model Uncertainty in Aerospace Systems, Massachusetts Institute of Technology, Cambridge, 2008.
[16] L.C. Shen, J. Chen, N. Wang, Overview of air vehicle mission planning techniques, Acta Aeronaut. ET Astronaut. Sin. 35 (3) (2014) 593–606.
[17] S. Rathinam, R. Sengupta, S. Darbha, A resource allocation algorithm for multivehicle systems with non-holonomic constraints, IEEE Tans. Autom. Sci. Eng. 4 (1) (2007) 98–104.
[18] S.S. Ponda, L.B. Johnson, A. Geramifard, et al., Cooperative mission planning for multi-UAV teams, in: Handbook of Unmanned Aerial Vehicles, Springer Netherlands, 2015, pp. 1447–1490.
[19] A. Tsourdos, B. White, M. Shanmugavel, Cooperative Path Planning of Unmanned Aerial Vehicles, John Wiley & Sons, 2010.
[20] B. Woosley, P. Dasgupta, Multi-robot task allocation with real-time path planning, in: Proc. of the Twenty-Sixth International Florida Artificial Intelligence Research Society Conference, 2013, pp. 574–579.
[21] A. Arsie, K. Savla, E. Frazzoli, Efficient routing algorithms for multiple vehicles with no explicit communications, IEEE Trans. Automat. Control 54 (10) (2009) 2302–2317.
[22] S. Moon, E. Oh, D.H. Shim, Integral framework of task assignment and path planning for multiple unmanned aerial vehicles in dynamic environments, J. Intell. Robot. Syst. 70 (1–4) (2013) 303–313.
[23] T. Erlandsson, L. Niklasson, Threat assessment for missions in hostile territory - from the aircraft perspective, in: International Conference on Information Fusion, IEEE, 2013, pp. 1856–1862.
[24] T. Erlandsson, L. Niklasson, Automatic evaluation of air mission routes with respect to combat survival, Inf. Fusion 20 (20) (2014) 88–98.
[25] Z. Peng, B. Li, X. Chen, et al., Online route planning for UAV based on model predictive control and particle swarm optimization algorithm, in: Intelligent Control and Aotomation, IEEE, 2012, pp. 397–401.
[26] Darrell Whitley, Doug Hains, Adele Howe, A hybrid genetic algorithm for the traveling salesman problem using generalized partition crossover, in: Proc of the 11th Int Conf on Parallel Problem Solving from Nature, Vol. 6283, Springer Heidelberg, Berlin, 2010, pp. 566–575.
[27] Zakir H. Ahmed, Zakir h ahmed genetic algorithm for the traveling salesman problem using sequential constructive crossover operator, Int. J. Biometrics Bioinform. 3 (6) (2010) 96–105.
[28] E.-G. Talbi, Metaheuristics: From Design To Implementation, Wiley, Hoboken, 2009.
[29] F. Glover, M. Laguna, Tabu search, Gen. Inf. 106 (2) (1997) 221–225.
[30] T. Erlandsson, L. Niklasson, A five states survivability model for missions with ground-to-air threats,spie defense, Secur. Sens. (2013) 875207.
[31] T. Erlandsson, L. Niklasson, A five states survivability model for missions with ground-to-air threats, in: Proceedings of SPIE, Modeling and Simulation for Defense Systems and Applications VIII, 8752, 2013, pp. 875207–1–875207–12.
[32] Chen Huagen, Wu Jiansheng, Wang Jialin, et al., Mechanism study of simulated annealing algorithm, J. Tongji Univ. (Nat. Sci.) 32 (6) (2004) 802–805.
[33] N.H. Quttineh, T. Larsson, Military aircraft mission planning, Optim. Lett. 9 (8) (2015) 1625–1639.

Qian Ning is now an Associate Professor in College of Electronics and Information Engineering, Sichuan University, Chengdu, 610065 China and in School of Physics and Electronics, Xinjiang Normal University, Urumqi, 830054 China. His current research interests include Wireless Ad hoc network and pattern recognition.

Guiping Tao is now a graduated student in the College of Electronics and Information Engineering, Sichuan University, Chengdu, 610065 China. Her current research interests include UAV trajectory and mission planning.

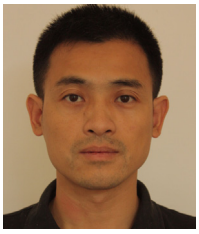

Bingcai Chen received his MS degree and Ph.D. degree in Information and Communication Engineering from Harbin Institute of Technology (HIT), Harbin, China, in 2003 and 2007, respectively. He has been a visiting scholar in University of British Columbia, Canada, in 2015.

He is now a professor in the school of computer science and technology at Dalian University of Technology, Dalian, China, and in the School of Computer Science and Technology, Xinjiang Normal University, Urumqi, China. His current research interests include UAV network and communication, network and information security, computer vision, etc.

He received National Science Foundation Career Award of China in 2009. He is severing as a reviewer for project proposals to National science foundation of China, Ministry of Education of China. He is also serving as a reviewer for some refereed Journals including IEEE Transaction on circuit and systems for video technology, Journal of Electronics, Journal of Communication, et al.

Yinjie Lei received his M.S. degree from Sichuan University (SCU), China, with the area of Image Processing in 2009, and the Ph.D. degree in Computer Vision from University of Western Australia (UWA), Australia in 2013. He is currently an associate professor with the college of Electronics and Information Engineering at SCU. He serves as the vice dean of the College of Electronics and Information Engineering at SCU since 2017. His research interests mainly include deep learning, 3D biometrics, object recognition and semantic segmentation.

Hua Yan received the B.S. degree in Automation, the M.S. degree in Radio Electronics, and the Ph.D. degree in Mechanical Automation from Sichuan University in 1993, 1996, and 2008, respectively. Currently, he is a professor with the College of Electronics and Information Engineering at Sichuan University. His research interests include pattern recognition and intelligent system.

Chengping Zhao is now an Associate Professor in College of Electronics and Information Engineering, Sichuan University, Chengdu, 610065 China. Her current research interests include pattern recognition, computer application, etc.